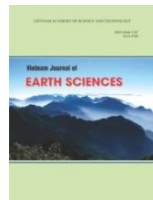




Vietnam Academy of Science and Technology

Vietnam Journal of Earth Sciences

<http://www.vjs.ac.vn/index.php/jse>



Direction of urban expansion in the Bangkok metropolitan area, Thailand under the impacts of a national strategy

Can Trong Nguyen^{1,2*}, Nguyen Thi Hong Diep¹, Sanwit Iabchoon³

¹*College of Environment and Natural Resources, Can Tho University, Vietnam*

²*Joint Graduate School of Energy and Environment (JGSEE), King Mongkut's University of Technology Thonburi (KMUTT). Center of Excellence on Energy Technology and Environment (CEE), PERDO, Ministry of Higher Education, Science, Research and Innovation, Thailand*

³*KMUTT Geospatial Engineering and Innovation Center, Faculty of Science, King Mongkut's University of Technology Thonburi, Thailand*

Received 6 June 2021; Received in revised form 04 July 2021; Accepted 15 August 2021

ABSTRACT

The Eastern Economic Corridor project (EEC), which spans over three coastal provinces east of the Bangkok Metropolitan Area (BMA), aims to transform Thailand into a developed country progressively. The EEC project promises to influence its territory and surrounding areas. We aimed to monitor the urbanized directions at the BMA during 2015-2017 and explore whether the BMA's urban expansion trend is related to the EEC. The results revealed that the built-up areas increased by 24,033 hectares (22.8%). The urban districts with high urban density slowly developed, while the rural districts tended to urbanize with a high urbanization rate, approximately 6.8% per year. The BMA urban areas mainly expanded to the east (14.9% per year) and southeast (21.6% per year) under partial impacts from the EEC infrastructure projects. The research findings represent a concept for assessing urban expansion and pointing to the regions of concern, which will be meaningful for urban planning and policymaking.

Keywords: Bangkok Metropolitan Area, Eastern Economic Corridor, urbanization dynamics, urban expansion, spatial analysis.

©2021 Vietnam Academy of Science and Technology

1. Introduction

Urbanization is an inevitable process when rural areas become towns and urban areas due to economic growth and industrialization (Peng et al., 2010; Rubiera Morollón et al., 2017). Like other big cities in Asia, Bangkok has been experiencing rapid urbanization with substantial investments in urban infrastructures and other public utilities

(Murakamia et al., 2005; Tsuchiya et al., 2015). Therefore, Bangkok has promptly become a megacity and a regional hub in the widespread globalization trend. The Gross National Products (GNP) reached approximately 40%, with only 10% of the total population (Keivani, 2010). Although the single Bangkok population accounts for a small percentage of the national population, its residents rapidly increased over six times through only six decades, from 1.4 million in 1950 to 10.15 million in 2018 (United

*Corresponding author, Email: can.62300800201@mail.kmutt.ac.th

Nations, 2018; Yamashita, 2017). As a result, the Bangkok urban areas also expanded from 26% (2000) to about 50% (2018) of the total provincial area (Song et al., 2021). Bangkok, therefore, became one of the five biggest cities in East Asia regarding urban areas (Deuskar et al., 2015). A study considering urbanization in Manila, Jakarta, and Bangkok revealed that Manila and Jakarta were in the early urbanization and suburbanization process. In contrast, Bangkok placed between these two stages with outward shifts in land use (Murakamia et al., 2005). In recent years, Bangkok and surrounding provinces - Bangkok metropolitan area (BMA) - have shown symptoms of urban sprawl through built-up expansion and vegetation narrowing (Nguyen et al., 2021b). Nevertheless, a question arises as to which directions the city has been expanding.

Since 2016, Thailand introduced the Eastern Economic Corridor development plan (EEC) and called for domestic and international investments. This project is a national strategy in the Thailand 4.0 scheme to release the economy from barriers induced by the Thailand 1.0, 2.0, and 3.0 schemes, which focused on agriculture, light industry,

and advanced industry, respectively. The Thailand 4.0 scheme also aims to drive economic development and reaffirm the national prestige in Southeast Asia (EECO, 2018; Keawko et al., 2018). The project areas are located in “the heart” of Thailand’s mainland, the eastern coastal provinces (i.e., Chachoengsao, Chonburi, and Rayong). This will be a manufacturing hub with complete infrastructures and primary investments in the economic pillars, including aviation, logistics, smart electricity, modern automotive, robotics, biotechnology, digital, and tourism (Fig. 1) (Bhrammanachote, 2019). Land use/land cover (LULC) in the EEC provinces has dramatically changed since the EEC’s inception, as urban areas have replaced agricultural lands. The LULC in the eastern provinces has a high probability of continuing to transform into urban and built-up areas (Tontisirin et al., 2017). The conversion is consistent with the land transformation that has rapidly happened in Chachoengsao province, with a significant increase in residential areas and manufacturing sites (Pruksanubal, 2016; Tontisirin et al., 2017). The EEC will boost the local areas and affect the development in the surrounding areas.

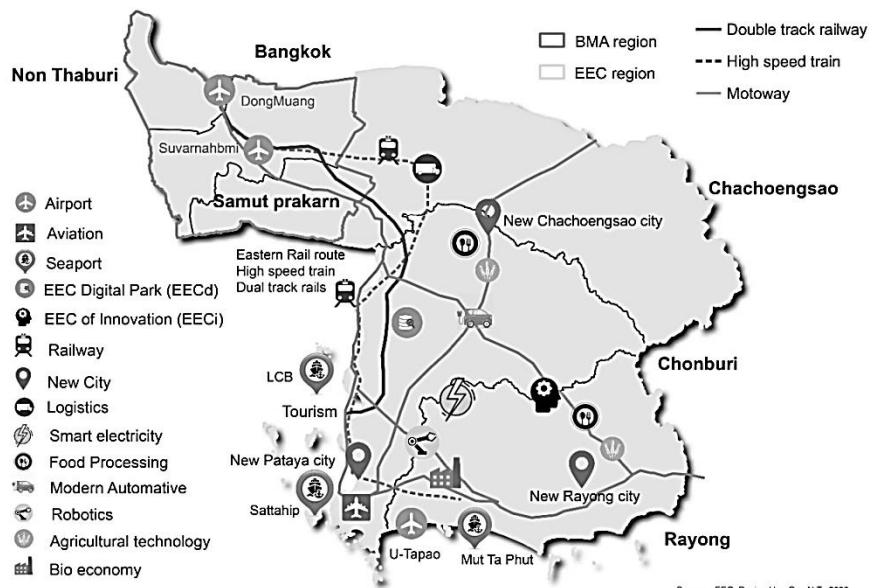


Figure 1. General infrastructure plans and principal sectors in the Eastern Economic Corridor.
The sketch was redrawn using aggregated data from diverse sources

Therefore, this study aimed to explore the land cover changes in the Bangkok Metropolitan Area throughout 2015-2017 to learn how the EEC impacts urbanization in a neighboring area when the project period has just started. More explicitly, we also detected primary directions of urbanization in BMA based on directional analyses and grouping approach using urban density and urbanization rates.

2. Research area and acquiring data

2.1. Research area

According to the Metropolitan Electricity Authority (MEA), Bangkok Metropolitan Area (BMA) comprises the Bangkok capital core, the Nonthaburi province in the northwest, and

Samutprakarn province in the southeast (MEA, 2016). There are 18 subdistricts that together constitute these three provinces (Fig. 2). We considered the three provinces instead of the greater Bangkok Metropolitan Region (BMR) directly linked to the EEC region. As a rapidly urbanized area, the BMA has expanded into suburbs around the capital and turned these areas into multiple unconnected peri-urban regions since the 1980s. These peri-urban areas are a mixture of urban and agricultural land use categories (Hara et al., 2008, 2005; Murakami et al., 2005; Tsuchiya et al., 2015). Nguyen et al. (2021b) stated that urbanization expressions in the BMA during 2015-2017. Therefore, this study intended to explore the direction of urban expansion in this area in the same period.

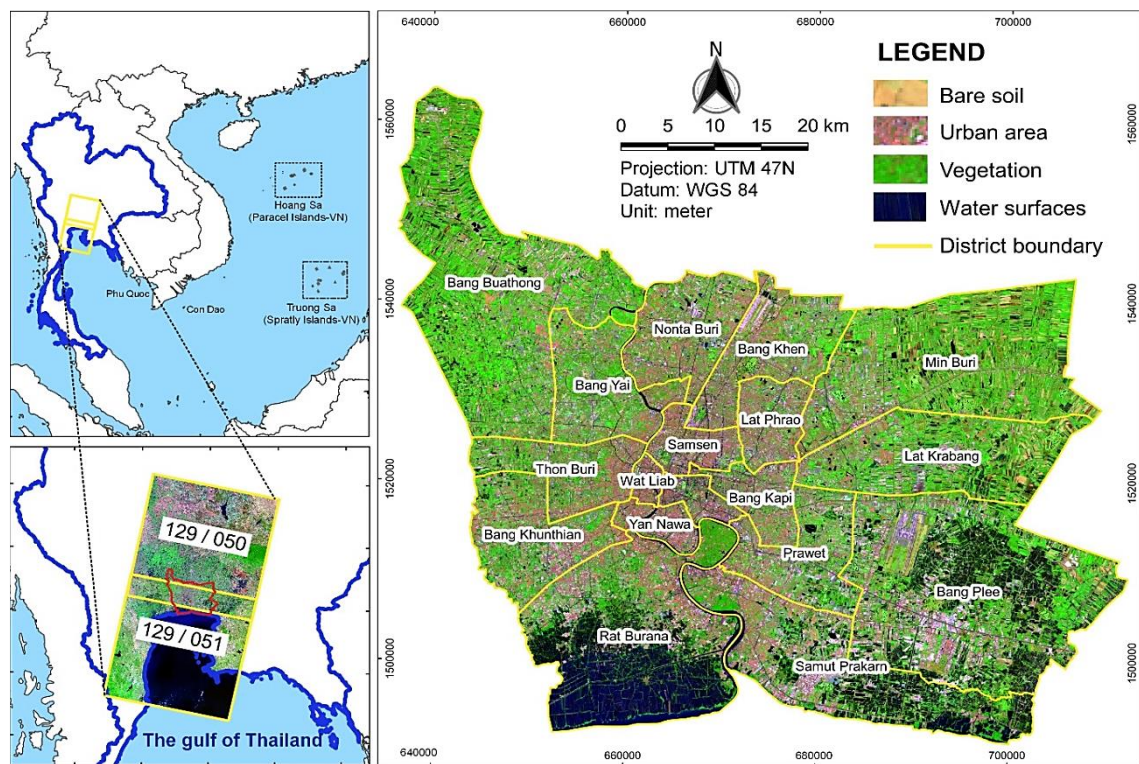


Figure 2. Map of Thailand in Southeast Asia, the two-scene position of collected Landsat imagery covers the entire research area and Landsat image inside the Bangkok metropolitan area. Landsat 8 (February 2015) is in false-color composite with bands SWIR/NIR/Green

2.2. Acquiring Data

The research utilized medium resolution remotely sensed data of Landsat imagery, which is available for online access at the U.S Geological Survey (USGS) website (<https://earthexplorer.usgs.gov>). We acquired the free-cloud images during the dry season to limit atmospheric and cloud effects on passive remote sensing data. The data consisted of Landsat 8 (OLI) in February 2015 and Landsat 7 (ETM+) in February 2017. Two scenes cover the entire study area each day, including the images with row/path of 129/050 and 129/051. The cloud rate of all images is less than 1.0 percent. Besides, the spatial resolution is 30 meters on multispectral bands and 15 meters on the Panchromatic band. This research used the Landsat 7 imagery because of a high cloud coverage of the Landsat 8 imagery in 2017 in this area. Although the Landsat 7 images have gaps error due to trouble on Scan Line Corrector (SLC) from 2003 onwards (Andrefouet et al., 2003), the retained information is still useful for many applications such as forest, land cover, and urban land use detection (Hu et al., 2016; Viet et al., 2014; Wulder et al., 2008). Thus, this study applied the gap-fill method to adjust the error data (detailed in a methodology section).

3. Methodology

3.1. Land cover classification

3.1.1. Data preprocessing

To achieve more accurate results, this research adopted a set of preprocessing procedures, with only resolution enhancement applied to the Landsat 8 images. In contrast, we preprocessed the Landsat 7 images using preprocessing steps involving resolution enhancement and gap filling to recover the missing data.

Gap filling on the Landsat 7 ETM+ imagery: We recovered the scan gaps on the

Landsat 7 imagery using the single-image digital number (DN) value by the interpolated triangulation method (Gautam et al., 2015; Miller et al., 2011; Molnar, 2016; Singh et al., 2015). The algorithm calculates each missing pixel value by the surrounding pixels with a moving window of triangles (Watson, 1992). Then, the “single file gap-fill (triangulation)” function on ENVI Gap-fill extension tool helps to corrects the gap errors.

Resolution enhancement: The Nearest-neighbor diffusion pan-sharpening assists to enhance the image's spatial resolution up to 15-meter by integration of multispectral bands (i.e., Red-Green-Blue-NIR-SWIR) and Panchromatic band (15 meters) (Sun et al., 2014). The final image is a multispectral image with a high detail scale of 15 meters. The high-resolution data helps to promote the classification ability of the Object-based Image Analysis (OBIA) algorithm.

3.1.2. Image Segmentation

Segmentation is an initial step in the OBIA classification, which groups individual pixels into distinct subsets. Each group of pixels is the same as the rest pixels in terms of spectrum and DN values. There are six bands used for the multi-resolution segmentation process, including three visible bands (Red-Green-Blue), Near Infrared (NIR) band, and two Shortwave Infrared (SWIR) bands (Jacquin et al., 2008). The parameters that significantly influence object size are scale, shape, and compactness (Duan et al., 2016). After the trial segmentation, the study obtained the segmental parameters when the land cover features can be clearly detected. The shape and compactness values are 0.1 and 0.5, respectively. The scale value on Landsat 7 imagery is 15, while it reaches 160 on Landsat 8 image. Landsat 7 data encoded in 8 bits, so the DN range is substantially narrow than the range on Landsat 8 data encoded in 12 bits.

3.1.3. Spectral Index calculation and Sampling

A spectral index is a powerful approach to detect land cover features on satellite imagery (Diep et al., 2019). In this study, we calculated three spectral indices representing vegetation, urban areas, and bare land. The study used Normalized Difference Vegetation Index (NDVI) for vegetation feature extraction (Tucker, 1979). The Normalized Difference Built-up Index (NDBI) improves discrimination between water surfaces and urban features (Bouhennache et al., 2015; Xinmin et al., 2017; Zha et al., 2003). Moreover, the Green-Red Vegetation Index (GRVI) is the crucial index for extracting bare soil via greening color. The spectral reflectance of a green wavelength is lower than the red wavelength spectral reflectance for bare soil (Falkowski et al., 2005; Motohka et al., 2010).

We selected training samples scattered and randomly on the segmented image based on reference data (truth points) and imagery characteristics (i.e., interpretation keys) that consist of color, tone, size, shape, texture, pattern, height, shadow, and associated relationships (Minh, 2010). The training samples are the well-known data for training the classification algorithm to assign classes for the rest of unknown pixel groups (Kumar, 2004). This study classified remotely sensed images into four land cover categories broadly utilized in urban-related studies, including the urban areas, vegetation, water bodies (i.e., hydrological system and aquaculture), and bare soil (Aboelnour and Engel, 2018; Ha et al., 2021; Mukherjee and Singh, 2020).

3.1.4. Rule-set based classification

Then, the study analyzed the selected samples to identify the index values range for different land cover categories. More explicitly, we considered the index distribution graphs of each land cover class on

each spectral index to determine the optimal thresholding values, a value range with the least overlapping area with other categories, to distinguish land covers from each other, shown in Table 1. Generally, the value range per index in different years is not entirely identical, and many driving forces lead to the observed variation. For example, the Landsat 7 images are in 8 bits with 256 gray levels because its acquired sensor is the ETM+. In comparison, the Landsat 8 images are in 12 bits, with 4,096 numeric values produced by the OLI-sensor. Besides, the additional elements such as the weather conditions, the solar radiation, and even cloud covering in surrounding areas also influence the DN values on the remotely sensed imagery. Subsequently, the study applied the Rule-set based method (i.e., a kind of decision tree) to classify land cover classes using the empirical values in Table 1. Firstly, the study separated vegetation from others by using NDVI. Next, NDBI assisted in extracting the water bodies, and the urban areas were finally distinguished from the bare soil areas using GRVI.

Table 1. Thresholding values for different spectral indices used in rule-set based classification

Index	2015	2017
NDVI	≥ 0.19	≥ 0.1
NDBI	≥ -0.4	≥ -0.045
GRVI	≥ -0.002	≥ 0.05

3.2. Accuracy assessment

The study assessed the classification performance by the overall accuracy and kappa (K) coefficient (Congalton, 1991; Congalton and Green, 2009). A confusion matrix constructed by comparing classified images and truth points is a principal data to estimate these metrics. In a confusion matrix, accurate points are on the diagonal, while the numbers on two halves of a triangle are misclassified points among the land cover types. Regular points function on a 2-square-kilometer grid generated a set of truth points to validate the classification results. There are a total of 794 points covering the entire study

area (Fig. 3). These points were then checked their land cover types in 2015 and 2017 by comparing very-high-resolution images (VHR) on Google Earth through Show historical imagery (Nguyen et al., 2021a; Tran

et al., 2017). Finally, the low-quality points because of cloud and unclear pixels were eliminated from the final truth point dataset, in which there are only 748 points in 2015 and 759 points (2017).

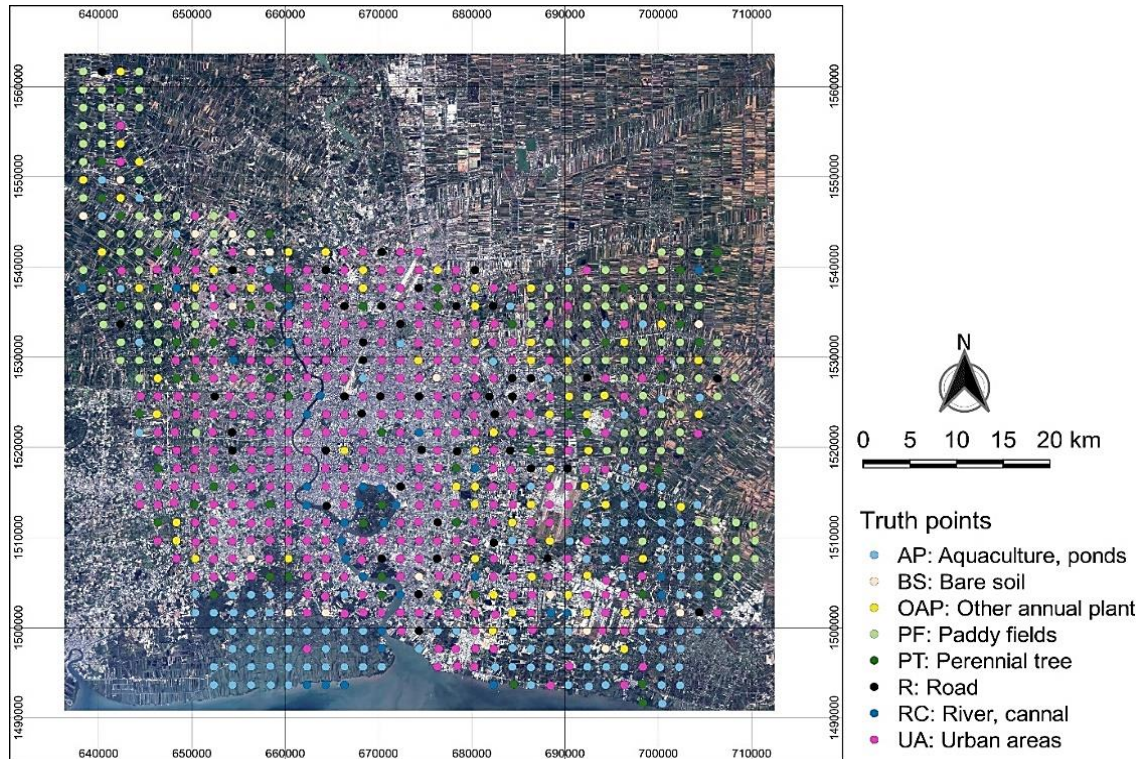


Figure 3. Truth points distribution on BMA Landsat background in true-color composite (RGB)

3.3. Calculation of urban-related indicators and Grouping method

The characteristics for classifying a town are urban or rural, which are relatively diverse, such as population, primary economic sectors, and urban areas. In this study, we calculated the development degree of a district via the urban density (UD), a ratio between the urban and total areas, as given in Equation (1). Besides, we evaluated the average urbanization speed (or urbanization intensity) by the urbanization rate. The annual urbanization rate (AUR) is a quotient of the additional urban area per year and the initial

urban area, using Equation (2) below (Ahmad and Goparaju, 2016).

$$UD = \frac{UA}{TA} \quad (1)$$

$$AUR = \frac{(UA_{end} - UA_{initial})}{N.UA_{initial}} \quad (2)$$

Where UD is the urban density of a specific town; UA is the urban area at the time of evaluation (Hectares); TA is the total area of the town (Hectares); AUR is the urbanization rate; UA initial is the urban area at the beginning of the period (Hectares); UA end is the urban area at the ending time of the

period (Hectares); N is the total years of evaluation (years).

The study assessed each district regarding urban density and urbanization rate. The reference value of these two indicators varies depending on the nations and regions. Therefore, this study suggested using median values (M_d) of the urban density and urbanization rate as a primary metric for classifying whether a district is rural or urban and its growth rate. The median lines of these two parameters divide the coordinate plane into four parts corresponding to four district groups with different patterns regarding urban density and urbanization rate. A district with a higher urban density than the median value is considered an urban district. In contrast, a district is assigned as a countryside county when its urban rate is lower than the median value. Likewise, the urbanization speed was explored by collating the urbanization rate and its median value. A rapidly urbanized district is supposed to own a higher urbanization rate than the median value, whereas a low rate regulates a slowly growing county.

3.4. Data visualization using rings map

The rings map technique visualized the urban density and yearly urbanization rate dataset in different geographical directions. The rings map is a powerful tool to illustrate many-year data layers of one object, in which each ring represents, in turn, a single year (Stewart et al., 2011). This study constructed the ring map by a QGIS extension tool programmed in python language (Lee, 2015). The tool creates a base map consisting of eight geographical directions around Bangkok's center ($13.736717^{\circ}\text{N}$; $100.523186^{\circ}\text{E}$) at the first stage. Each polygon attribute information is direction, urban density in 2015, urban density in 2017, and the annual urbanization rate. Subsequently, the extension constructed

spokes around the base map and anchor line to connect a spoke with a corresponding polygon (Fig. 4). The attribute values place on different rings of the spoke. The number of rings and spokes is equal to the amount of attribute information and polygons shown.

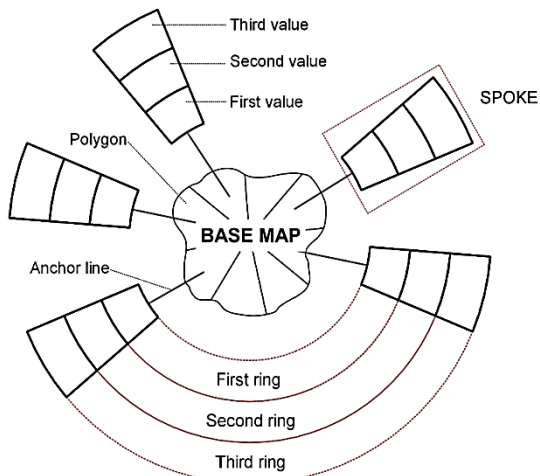


Figure 4. Diagram of ring map elements

The primary direction of urban growth was analyzed using the Standard Deviational Ellipse (SDE). The highest urban density locates inside an ellipse, whereas a dominated expansion pathway is the direction along a major axis. The SDE is the typical approach for measuring the trend of a dataset by calculating the standard distance in the x and y axes, which was put into practice to explore the spatial distribution of educational services, conferences, visitors, and impervious surfaces (Alananze et al., 2018; El-borsh et al., 2017; Korpilo et al., 2018; Qiao et al., 2017). The standard ellipse was drawn based on the major and minor axes, a standard deviation of x and y compared to the mean center of the urban area (ESRI, 2016). In this research, we applied a one-standard deviation corresponding to nearly 68% of the data distribution to analyze urban district density (Kazmier, 2003).

4. Results

4.1. Urban land cover changes

The object-oriented image classified results are generally evaluated via a confusion matrix when comparing to the true points. The classified land cover achieved an almost perfect acceptance within all cases (Viera and Garrett, 2005). The kappa coefficient in 2015 and 2017 are 0.86 and 0.85, respectively, corresponding to the matched points between the classified result and validated points were 679 points (2015) and 684 points (2017) points. Despite the slight disparity, the classification still reached a righteous requirement to extract urban areas for urban development analysis.

The land cover in BMA includes four types such as urban areas, vegetation, water bodies, and bare soil. The urban areas are

impervious surfaces (e.g., houses, buildings, asphalt roads). The urban areas are highly concentrated in the city core and spread away from other sides, following the primary traffics and hydrological systems. The vegetation (or agricultural areas) is green spaces such as paddy fields, vegetable fields, orchards in the countryside, parks, lawns in the city, and mangrove forests along the southern seashore. The water surfaces consist of the Chao Phraya River as the main river flowing through “the heart” of the capital and other surrounding tributaries. Besides, lakes and wetlands are randomly distributed throughout the study site, while aquaculture ponds are in the coastal areas of Ratburana and Samut Prakarn districts. Finally, most of the bare soil is the harvested fields located in suburban districts of Bangbuathong, Minburi, and Ladkrabang (Fig. 5).

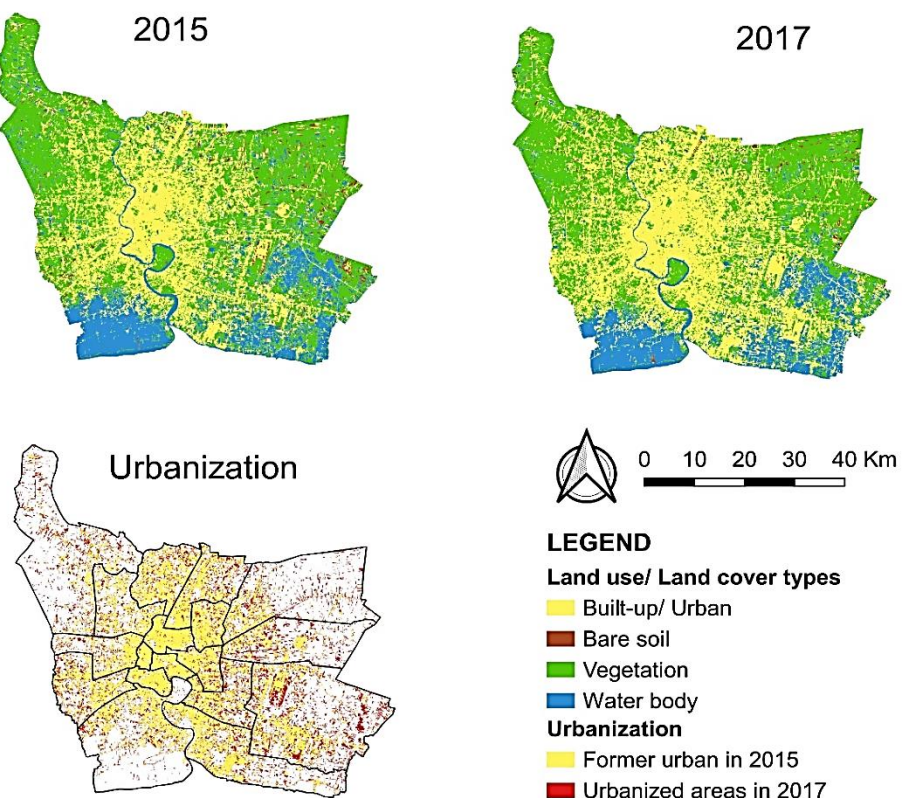


Figure 5. Land cover maps in 2015 and 2017 classified by Landsat satellite imagery, and urbanization of the Bangkok Metropolitan during the observed period

Figure 6 shows the land cover area and its proportion. Vegetation was a dominant land cover in 2015, which accounted for 45.4% of the total area, with 143,569 hectares. These next land cover types were the urban areas, 105,391 hectares (33.3%), water surfaces, approximately 58,981 hectares (18.6%), and 2.7% of bare soil, regarding 8,590 hectares. The first tendency of the seasonal land cover types, including vegetation, water surfaces, and bare soil, was reduced in total area, which decreased by 14,951 hectares, 4,244 hectares, and 4,837 hectares, respectively. Oppositely,

the urban areas expanded and reached 129,424 hectares in 2017, which increased by 24,033 hectares, approximately 22.8%, compared to the urban area in 2015. Therefore, the urban area became the new dominance when its proportion achieved 40.9%, and the vegetation was only 40.6% of the land cover structure. The primary dynamic of urban sprawl was the gradual narrowing of agricultural land (4.8%). The bare soil transformed the rest urban area under construction, approximately 1.5% of the bare soil area.

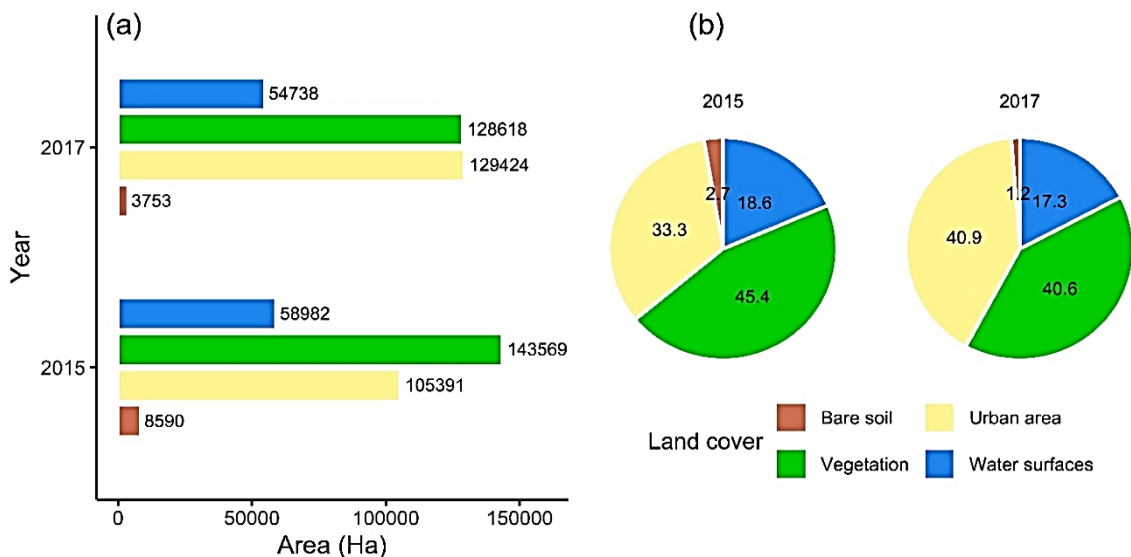


Figure 6. Graphs illustrate (a) total area and (b) proportion of land cover categories in 2015 and 2017

4.2. Urban expansion Analysis

4.2.1. Urban density and Urbanization rate

The urban density and urbanization rate revealed both the urban concentration and the level of urban development. The urban areas were mainly in the city center, and the urban density was inversely proportional to the distance to the city center. The urbanization rate was the opposite, where the districts further from the downtown had higher urbanization speed, especially the eastern districts.

The 18 districts in BMA constitute four individual groups representing four different levels of urban concentration and urbanization rate (Fig. 7a). Figure 7b shows four groups, including low developing urban districts, high developing urban districts, low developing countryside districts, and high developing countryside districts. First, the urban districts with low development, where the urban density was higher than 47.8%, and the urbanization rate was lower than 6.8% per year. Within this group, the downtown districts with over 80% area of the urban

areas, namely Yan Nawa (83.3%), Klong Toei (87%), Samsen (88.4%), and Wat Liab (89.1%). These districts had dense construction density and less potential for urban expansion. Hence, the urbanization rate in these inner districts was always lower than 2% per year. Next, Bang Khen was an urban district with high development where the urban density and urbanization rates were approximately 55.3% and 7.6% per year, respectively. Finally, the urban density of Bang Yai was 47.1%, and its yearly urbanization rate was 1.0%. Thus, Bang Yai was considered a countryside district with a

low development rate. The final group represents the countryside districts with high development. This group's general attributes are that these districts had low urban density, about 14.7-47.2%. Plus, the annual urbanization rate was higher than these other groups, which achieved 11.2% per year up to 30.5% per year. Highlights were three eastern countryside districts, Prawet, Lat Krabang, and Bang Plee, with the yearly urbanization rate reaching 16.1%, 20.8%, and 30.5%. Thus, most urban districts slowly developed, whereas most rural districts tended to expand urban areas speedily.

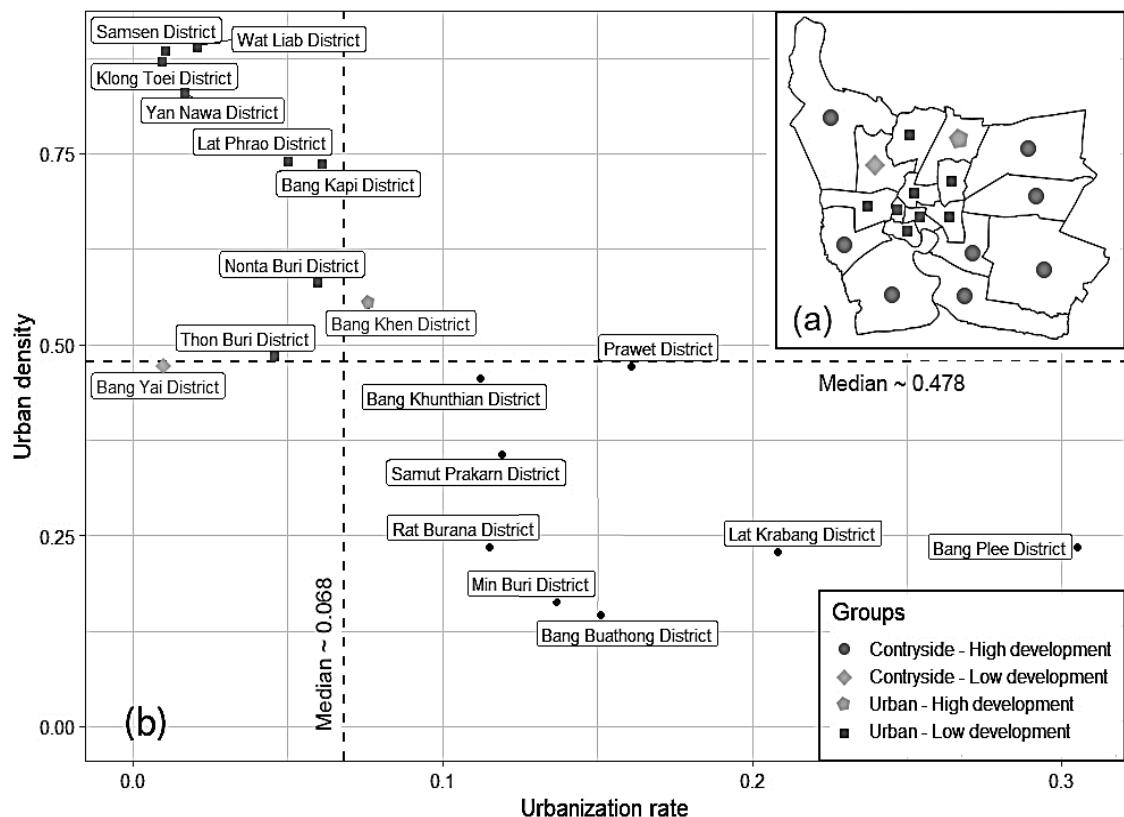


Figure 7. The figure illustrates district grouping (a) spatial distribution of eighteen districts and (b) 2D graph basing on urban density and annual urbanization rate. Colors of legend text correspond to the colors of district groups

4.2.2. The direction of urban sprawl

Regarding directional urban concentration, the study revealed a growth in the urban

density over the years in every geographical direction (Fig. 8). The directions have densely developed with an urban concentration higher

than the median value in 2015 ($Md = 37.5\%$) were the northeast (37.6%), the southwest (39.7%), the west (44.1%), and the north (54.6%). Among these directions, the development in most directions was relatively low. An annual rate of less than 8.6%, except the southwest, reached an average rate of 9.1% per year and considered a moderate-high development direction. Although the south, the southeast, and the east had a low level of urban concentration, there was considerable development in these three directions, with the annual rate of 8.7%, 14.9%, and 21.6%, respectively. The profoundly isolated development was in the northwest, with low urban concentration and urbanization. The urbanization rate was lower than the median

value of $Md = 8.6\%$. The BMA has expanded in all directions over the years. However, the most robust development was recognized eastwards. Moreover, the SDE revealed this eastern expansion. The general ellipse in the whole period of 2015-2017 (red ellipse) has a major axis that deviates to the southeast indicating the principal direction for urban sprawl. Compared to 2015 (green ellipse), the standard deviation ellipse in 2017 (blue ellipse) deforms and enlarges its major axis length towards the east as an eastern suburbanization expression. On the contrary, the north's urban development was moderate because the north's urban spaces were already compact, and thus, the urban development in this direction seemed unlikely to expand.

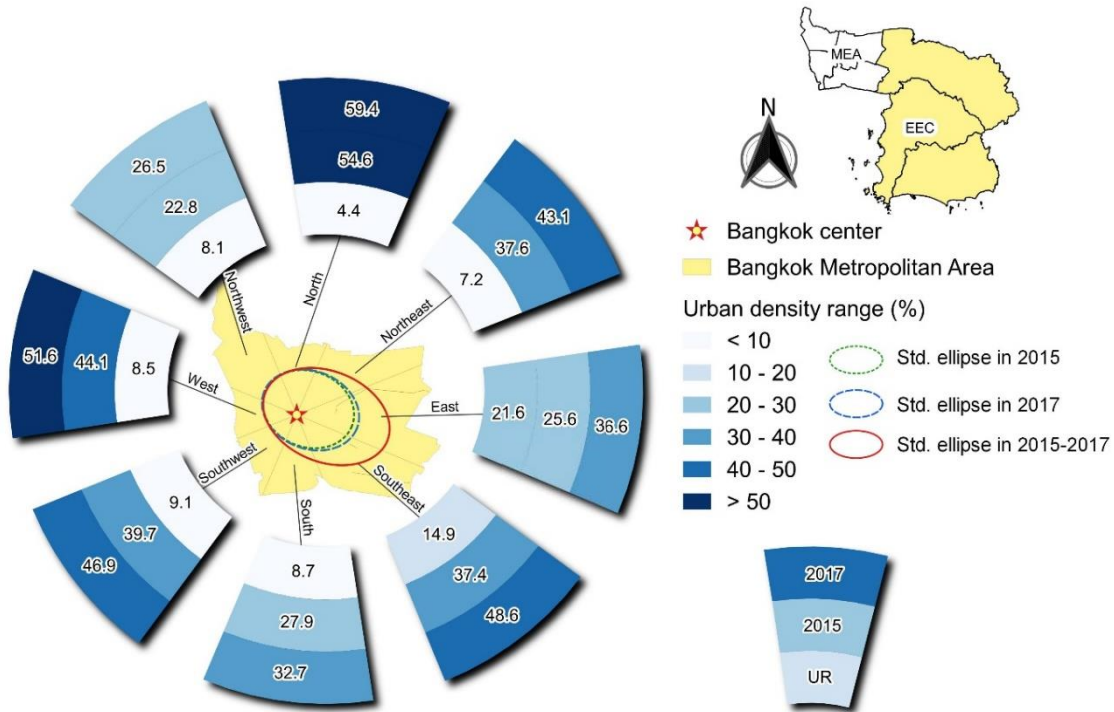


Figure 8. Rings map demonstrates the annual urbanization rate and urban density in 2015 and 2017 in geographical directions. The spatial standard deviation ellipses illustrate the trend of urban development in the corresponding years

5. Discussions

5.1. Urban sprawl dynamics

After moving the ancient capital from the west to the east of the Chao Phraya River in the 1780s, the Bangkok capital (or “Krung Thepmahanakorn”) has been expanding to the outer surrounding districts (i.e., peri-urban areas) as a suburbanization process and becoming a regional hub (Jongkroy, 2009). The local authority initiated comprehensive planning to pursue the suburbanization process. The industrial zones and post-harvest plants help relieve the inner city’s pressures due to the dense distribution of other urban infrastructures outside the city and close to raw materials (MLIT, 2013; Nakagawa, 2004; Pansuwan and Routray, 2011). Our findings provide convincing evidence of suburbanization in the surrounding rural districts, commonly cited as the urbanized hotspot with a high development rate.

The spatial analysis and data visualization revealed that the urban sprawl had been swiftly

moving towards the eastern directions, i.e., the east and the southeast. Figure 9 is an additional analysis of urban expansion rate in the eastern BMA and EEC provinces during 2010-2018, showing that the urban sprawl in the eastern BMA was closely related to the urbanization process in EEC regions ($R^2 = 0.98$). Although the EEC’s urban expansion rate was higher than eastern BMA, the developing tendency was comparable, and it significantly increased since 2016 (i.e., time of the EEC strategy’s enactment). The potential for urban expansion and partially by the effect of the EEC project at the first stage, which the Thailand Government launched to revitalize and enhance various industry productions, is a primary driving force of urbanization on the east side of BMA (EECO, 2018; Koen et al., 2018; Tontisirin et al., 2017). For example, six pilot infrastructure projects started in 2017. A “high-speed rail project” connecting three airports (Suvarnabhumi, Don Mueang, and U-Tapao) impacts the east BMA the project goes through.

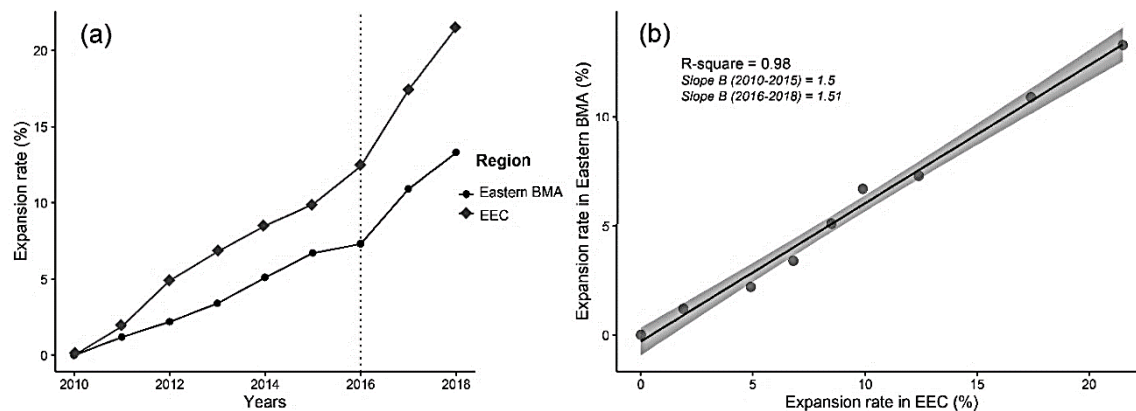


Figure 9. (a) Trend chart presents the urban expansion rate in the eastern BMA and EEC region in 2010-2018, and (b) linear regression graph of eastern BMA expansion rate depends on the expansion rate in EEC

The EEC project bases on the public-private partnerships in which the government conducts the land clearance and handovers to private investors with “super-generous

incentives” and investment facilitation. For example, Bhrammanachote (2019) mentioned incentives for foreign direct investment (FDI) in EEC, including tax exemption, free-trade,

non-tax area, and land renting time for 50+49 years. The land cover in the three EEC provinces has been dynamic because of land clearance at the project's initial stage. Besides, the Infrastructure Development Implementation Programs (IDIP) and several important transportation infrastructure development projects (TIDP) encourage the connections between the EEC new cities, industrial centers, and the excellent capital region (EECO, 2018). Thus, the EEC not only owns the favorable conditions itself for the development, but it also promotes the development in contiguous areas, chiefly the eastern of the BMA.

The elements, including population, economic conditions, industrialization, and education, drive urbanization in developing countries. Therefore, these quantitative factors are important predictor variables in the urbanization model (Guangjin et al., 2016; Hofmann and Wan, 2013; Kuang et al., 2014). Nevertheless, the political and policy factors such as urban planning, management strategies, and policies forcefully affect urbanization by adjusting other drives (Kuang et al., 2014; Thanh, 2007).

5.2. Implications of urban planning

The post-classification detection method is a typically applied approach to detect land cover changes and urban changes. The method is described as a GIS-based overlaying technique on the layers and cross-tabulation to construct a change matrix of gains and losses (Hegazy and Kaloop, 2015; Rawat and Kumar, 2015; Tolessa et al., 2017). Then, gradient analysis (i.e., consideration of urban area change in concentric circles) and zonal analysis (Ahmad and Goparaju, 2016; Ramachandra et al., 2015) are well-known approaches for urban expansion analyses. These tools help to thoroughly understand the urban growth at the local level and even the driving agent of changes. This research

combined the zonal-direction analysis and standard deviation ellipse to visualize the urban expansion in each direction and the principal directions of urban growth over the years. The research also implies an efficient approach to monitoring and evaluating the master plan by assessing the urban expansion using directional analysis. Besides, the integrated grouping based on urban density and urbanization rate is another method to assess the local development the method simultaneously located the districts with potential problems during urbanization performance. Notably, the low development districts amongst the global growth should be especially considered during the urban plan, mainly depending on its inherent problems. The countryside district with a high urbanization rate is a fast-developing district with high ability expansion. Hence the aspects that should consider including necessary investments, completion of urban infrastructures, and appropriate urban planning. On the other hand, the countryside district with a low urbanization rate is typically a district facing several impediments for urbanization. Therefore, further investigations should conduct to understand the key constraints and solutions better. In contrast, the common burdens in an urban district with high urbanization rates are public green space areas, wastewater treatment, the loading capacity of infrastructures, and urban designs (i.e., The heterogeneity of the urban landscapes, for instance, the difference between modern skyscrapers against degraded apartments or houses within a city).

5.3. Risks and challenges

The EEC is a national priority project. When completed, this project will help drive economic development and Thai society to rise to a developed country quickly (EECO 2018). The EEC implied multi-disciplinary infrastructures. However, several potential

problems still need to be addressed at the early stage of a new-great project. These difficulties include international investment policy, land policy, land use transformation and planning, environmental concerns, and social aspects. At a newly forming metropolitan, land use transformation and real estate market are dynamic (e.g., Chachoengsao province) (Pruksanubal, 2016). Hence, these conditions favorably bridge the land speculation and chaos in the real estate market (Manotham, 2010). Establishing a completely new metropolitan from a countryside area is more accessible than renovated planning regarding the land fund and spatial distribution planning. Nevertheless, spatial planning should be finalized and evaluated for its long-term impacts. A few elements should be considered in the renovated planning, such as maintenance of natural resources, green spaces, increase urban heat island, potentials of environmental pollution, and backup solutions (Aman et al., 2019; Can et al., 2019; Nitivattananon and Srinonil, 2019; Shen et al., 2008; Son et al., 2020, 2017; Son and Thanh, 2018).

Concerning social aspects, the rapid shift in economic structure from agriculture to industry at the planned region will effortlessly imply the social risks and the resistances for the general development, listed as unemployment, qualified labor, and career transition. Less-educated farmers, women, and middle-aged rural laborers will be the most vulnerable subjects who own low adaptive capacity in the urban labor markets (Heurlin, 2019; Shouhai, 2015). Therefore, developing national strategies for livelihood stabilization, training, and career transition support in the planned areas and even potentially affected as eastern of BMA. The EEC will be a comprehensively sustainable metropolitan, economically, environmentally,

and socially when efficiently addressing these social risks.

5.4. Current limitations and Outlooks

Although this study completed several tasks, which implies both methodology and hints for urban planning, there are still a few gaps that should be considered. We showcased a simpler framework to evaluate urbanization by grouping urban density and urbanization rate and directional analyses. Yet, the data for these analyses come from the OBIA. Basic users (e.g., planners and decision-makers) may find difficulties because its procedure is dissimilar to conventional classification methods. The performance is also relatively low, especially for segmentation. The google earth engine (GEE) could be applied to take advantage of its data and machine learning algorithms for image interpretation. Besides, the study utilized enhanced resolution images from Landsat (15 meters). The resolutions could improve by using Sentinel-2 and other commercial sensors. As a result, the classification accuracy will significantly improve. Also, we only considered urbanization in terms of spatial expansion while socioeconomic aspects have yet been included within this study. Nevertheless, urban infrastructures are always deployed before “rural-urban migration waves” and economic growth. A comprehensive analysis of these three aspects (i.e., urban area, population, and economic indicators) will provide a multidimensional picture of urbanization for effective planning and management.

6. Conclusions

This study presents the BMA urbanization tendency from 2015 to 2017 using spatial analysis and data visualization approaches. First, we classified the land cover data from the earth observation data, which all achieved

K>0.85. Then, the study utilized remote sensing-based data to analyze the urbanization tendency. The urban area in the BMA shifted from 105,391 to 129,424 hectares, corresponding to the urban proportion in land cover structure of 33.3% and 40.9% in 2015 and 2017, respectively. The two indicators of urban density and urbanization rate provide information for urban concentration and urbanization assessment. The BMA urban densely concentrated in the inner districts, especially in the northern district, compared to the city center. The urbanization trend was a suburbanization process in every district and direction, whereas the countryside districts and eastern regions were the dramatic expansion with an annual urbanization rate of 6.8% and 14%, respectively. This trend is consistent with the suburbanization process historical evidence, present dynamics, and the EEC's renovated planning. Although the EEC project mainly focuses on the three eastern coastal provinces instead of the BMA, it has eventually promoted development in the eastern BMA through the connective infrastructures.

We adopted another integrated approach based on spatial analysis and data analysis to evaluate the EEC's urban sprawl and effects on neighboring areas. The framework helps to explain urbanization trends efficiently and even detecting concerned districts based on the urbanization indicators. The districts with distinctive development patterns were detected more explicitly, which were the managers' hints to address the existing obstacles. The research proposed policy solutions in three main groups based on urbanization status. The solutions are to deeply consider and address obstacles to urbanization in low-developed countryside districts. In high-developed districts, attention to general planning and the occupation transformation policies is critical, while the environmental policies for high-developed

urban districts should be carefully considered, especially for infrastructures and green spaces.

Acknowledgments

This study was performed in KMUTT Geospatial Engineering and Innovation Center, Faculty of Science, King Mongkut's University of Technology Thonburi, Thailand. We would also like to thank the National Science and Technology Development Agency for funding support. We would also like to show our gratitude to the Landsat 7-8 image courtesy of the U.S. Geological Survey. Furthermore, our gratitude extends to Dr. Pariwate Varnakovida for his critical comments throughout this research completion. Finally, our gratitude extends to the anonymous reviewers for their valuable comments.

References

- Aboelnour M., Engel B.A., 2018. Application of Remote Sensing Techniques and Geographic Information Systems to Analyze Land Surface Temperature in Response to Land Use/Land Cover Change in Greater Cairo Region, Egypt. *J. Geogr. Inf. Syst.*, 10, 57-88. <https://doi.org/10.4236/jgis.2018.101003>.
- Ahmad F., Goparaju L., 2016. Analysis of Urban Sprawl Dynamics Using Geospatial Technology in Ranchi City, Jharkhand, India. *J. Environ. Geogr.*, 9, 7-13. <https://doi.org/10.1515/jengeo-2016-0002>.
- Alananzeh O., Maaiah B., Al-Badarneh M., Al-Shorman A., 2018. The geographic distribution of conferences in Jordan from 2014 to 2016 using predictive GIS modeling. *J. Conv. Event Tour.*, 19, 167-185. <https://doi.org/10.1080/15470148.2017.1406832>.
- Aman N., Manomaiphiboon K., Pengchai P., Suwanathada P., Srichawana J., Assareh N., 2019. Long-term observed visibility in eastern Thailand: temporal variation, association with air pollutants and meteorological factors, and trends. *Atmosphere (Basel)*, 10. <https://doi.org/10.3390/atmos10030122>.
- Andrefouet S., Bindschadler R., Brown De Colstoun E.C., Choate M., Chomentowski W., Christopherson

- J., Doorn B., Hall D.K., Holifield C., Howard S., Kranenburg C., Lee S., Masek J.B., Moran M., Mueller-Karger F., Ohlen D., Palandro D., Price J., Qi J., Reed B., Samek J., Scaramuzza P., Skole D., Schott J., Storey J., Thome K., Torres-Pulliza D., Vogelmann J., Williams D.L., Woodcock C., Wylie B., 2003. Preliminary Assessment of the Value of Landsat 7 ETM+ Data following Scan Line Corrector Malfunction.
- Bhrammanachote W., 2019. The Review of Thailand's Eastern Economic Corridor: Potential and Opportunity. Local Adm. J., 12, 73-86.
- Bouhennache R., Boudin T., Taleb A.A., Chaddad A., 2015. Extraction of urban land features from TM Landsat image using the land features index and Tasseled cap transformation [WWW Document]. Recent Adv. Electroscience Comput. URL <http://www.inase.org/library/2015/barcelona/bypaper/ELECTR/ELECTR-22.pdf>.
- Can N.T., Diep N.T.H., Iabchoon S., Varnakovida P., Minh V.Q., 2019. Analysis of Factors Affecting Urban Heat Island Phenomenon in Bangkok Metropolitan Area, Thailand. VNU J. Sci. Earth Environ. Sci., 35, 53-62. <https://doi.org/10.25073/2588-1094/vnuees.4355>.
- Congalton R.G., 1991. A review of assessing the accuracy of classifications of remotely sensed data. Remote Sens. Environ., 37, 35-46. [https://doi.org/10.1016/0034-4257\(91\)90048-B](https://doi.org/10.1016/0034-4257(91)90048-B).
- Congalton R.G., Green K., 2009. Assessing the Accuracy of Remotely Sensed Data: Principles and Practices, Second edi. ed, The Photogrammetric Record. Taylor & Francis Group. https://doi.org/10.1111/j.1477-9730.2010.00574_2.x.
- Deuskar C., Baker J.L., Mason D., 2015. East Asia's Changing Urban Landscape: Measuring a decade of spatial growth. World Bank Publications, Washington DC.
- Diep N.T.H., Korsem T., Can N.T., Phonphan W., Vo Quang Minh, 2019. Determination of aquaculture distribution by using remote sensing technology in Thanh Phu district, Ben Tre province, Vietnam. Vietnam J. Sci. Technol. Eng., 61, 35-41. [https://doi.org/10.31276/VJSTE.61\(2\).35-41](https://doi.org/10.31276/VJSTE.61(2).35-41).
- Duan P. Van, Thin V.T., Huy N.Q., 2016. Estimated value of the object-oriented optimal segmentation parameters within ecognition software: Experiments in satellite images SPOT6. J. For. Sci. Technol., 6, 18-30.
- ECCO, 2018. Eastern Economic Corridor Office Website [WWW Document]. URL <https://www.ecco.or.th/en> (accessed 9.9.19).
- El-borsh S.H., El-mewafi M., Zarzoura F., 2017. Studying and Evaluating the Development axis in Damietta Governorate based on Geographic Information System (GIS). Int. J. Sci. Eng. Res., 8, 1726-1736.
- ESRI, 2016. How Directional Distribution (Standard Deviations Ellipse) works [WWW Document]. Environ. Syst. Res. Institute, Inc. URL <http://desktop.arcgis.com/en/arcmap/10.3/tools/spatial-statistics-toolbox/h-how-directional-distribution-standard-deviation.htm> (accessed 5.7.18).
- Falkowski M.J., Gessler P.E., Morgan P., Hudak A.T., Smith A.M., 2005. Characterizing and mapping forest fire fuels using ASTER imagery and gradient modeling. For. Ecol. Manage., 217, 129-146. <https://doi.org/10.1016/j.foreco.2005.06.013>.
- Gautam V.K., Gaurav P.K., Murugan P., Annadurai M., 2015. Assessment of Surface Water Dynamics in Bangalore Using WRI, NDWI, MNDWI, Supervised Classification and K-T Transformation. Aquat. Procedia Int. Conf. water Resour. Coast. Ocean Eng. (ICWRCOE 2015), 4, 739-746. <https://doi.org/10.1016/j.aqpro.2015.02.095>.
- Guangjin T., Xinliang X., Xiaojuan L., Lingqiang K., 2016. The Comparison and Modeling of the Driving Factors of Urban Expansion for Thirty-Five Big Cities in the Three Regions in China. Adv. Meteorol. <https://doi.org/10.1155/2016/3109396>.
- Ha L.T.T., Trung N. Van, Lan P.T., Ai T.T.H., Hien L.P., 2021. Impacts of urban land cover change on land surface temperature distribution in Ho Chi Minh city, vietnam. J. Korean Soc. Surv. Geod. Photogramm. Cartogr., 39, 113-122. <https://doi.org/10.7848/ksgpc.2021.39.2.113>.
- Hara Y., Takeuchi K., Okubo S., 2005. Urbanization linked with past agricultural landuse patterns in the urban fringe of a deltaic Asian mega-city: A case

- study in Bangkok. *Landsc. Urban Plan.*, 73, 16-28. <https://doi.org/10.1016/j.landurbplan.2004.07.002>.
- Hara Y., Thaitakoo D., Takeuchi K., 2008. Landform transformation on the urban fringe of Bangkok : The need to review land-use planning processes with consideration of the flow of fill materials to developing areas. *Landsc. Urban Plan.*, 84, 74-91. <https://doi.org/10.1016/j.landurbplan.2007.06.009>.
- Hegazy I.R., Kaloop M.R., 2015. Monitoring urban growth and land use change detection with GIS and remote sensing techniques in Daqahlia governorate Egypt. *Int. J. Sustain. Built Environ.*, 4, 117-124. <https://doi.org/10.1016/j.ijsbe.2015.02.005>.
- Heurlin C., 2019. Unemployment among land-losing farmers in China: Evidence from the 2010 census. *J. Contemp. China*, 28, 434-452. <https://doi.org/10.1080/10670564.2018.1542223>.
- Hofmann A., Wan G., 2013. Determinants of urbanization, ADB Economics Working Paper Series. Manila, Philippines. <https://doi.org/10.2139/ssrn.2295736>.
- Hu T., Yang J., Li X., Gong P., 2016. Mapping urban land use by using landsat images and open social data. *Remote Sens.*, 8. <https://doi.org/10.3390/rs8020151>.
- Jacquin A., Misakova L., Gay M., 2008. A hybrid object-based classification approach for mapping urban sprawl in periurban environment. *Landsc. Urban Plan.*, 84, 152-165. <https://doi.org/10.1016/j.landurbplan.2007.07.006>.
- Jongkroy P., 2009. Urbanization and changing settlement patterns in Peri-urban Bangkok. *Kasetsart J. - Soc. Sci.*, 30, 303-312.
- Kazmier L., 2003. Schaum's Outline of Business Statistics.
- Keawko W., Thanasing T., Suwanmanee A., 2018. Thailand Economic with Eastern Economic Corridor Development. *J. MCU Alumni Assoc.*, 7, 35-42.
- Keivani R., 2010. A review of the main challenges to urban sustainability. *Int. J. Urban Sustain. Dev.*, 1, 5-16. <https://doi.org/10.1080/19463131003704213>.
- Koen V., Asada H., Rizwan M., Rahuman H., 2018. Boosting productivity and living standards in Thailand. *OECD Econ. Dep. Work. Pap.* <https://doi.org/10.1787/e525c875-en>.
- Korpilo S., Virtanen T., Saukkonen T., Lehvävirta S., 2018. More than A to B: Understanding and managing visitor spatial behaviour in urban forests using public participation GIS. *J. Environ. Manage.*, 207, 124-133. <https://doi.org/10.1016/j.jenvman.2017.11.020>.
- Kuang W., Chi W., Lu D., Dou Y., 2014. A comparative analysis of megacity expansions in China and the U.S.: Patterns, rates and driving forces. *Landsc. Urban Plan.*, 132, 121-135. <https://doi.org/10.1016/j.landurbplan.2014.08.015>.
- Kumar M., 2004. Digital image processing, in: Sivakumar M.V.K., Roy P.S., Harmisen K., Saha S.K. (Eds.), *Satellite Remote Sensing and GIS Applications in Agricultural Meteorology*. World Meteorological Organisation, Switzerland, 81-102.
- Lee M., 2015. Create Ring Maps.
- Manotham P., 2010. Bangkok Urban Dynamics and Housing Market. Stockholm Royal Institute of Technology.
- MEA, 2016. Sustainability Report 2016. Move forward to Smart Metro. Bangkok metropolis.
- Miller R.L., Liu C.C., Buonassisi C.J., Wu A.M., 2011. A multi-sensor approach to examining the distribution of total suspended matter (TSM) in the Albemarle-Pamlico Estuarine System, NC, USA. *Remote Sens.*, 3, 962-974. <https://doi.org/10.3390/rs3050962>.
- Minh V.Q., 2010. *Remote sensing Technology*. Can Tho Univeristy Publishing House.
- MLIT, 2013. An overview of Spatial policy in Asian and European Countries [WWW Document]. Minist. Land, Infrastructure, Transp. Tour. (MLIT), Japan. URL. http://www.mlit.go.jp/kokudokeikaku/international/pw/general/thailand/index_e.html (accessed 10.2.18).
- Molnar G., 2016. Analysis of land surface temperature and ndvi distribution for budapest using Landsat 7 ETM+ data. *Acta Climatol. Chorol.*, 49-50, 49-61.
- Motohka T., Nasahara K.N., Oguma H., Tsuchida S., 2010. Applicability of Green-Red Vegetation Index for remote sensing of vegetation phenology. *Remote Sens.*, 2, 2369-2387. <https://doi.org/10.3390/rs2102369>.

- Mukherjee F., Singh D., 2020. Assessing Land Use-Land Cover Change and Its Impact on Land Surface Temperature Using LANDSAT Data: A Comparison of Two Urban Areas in India. *Earth Syst. Environ.*, 4, 385-407. <https://doi.org/10.1007/s41748-020-00155-9>.
- Murakamia A., Zain A.M., Takeuchi K., Tsunekawa A., Yokota S., 2005. Trends in urbanization and patterns of land use in the Asian mega cities Jakarta, Bangkok, and Metro Manila. *Landsc. Urban Plan.*, 70, 251-259. <https://doi.org/10.1016/j.landurbplan.2003.10.021>.
- Nakagawa S., 2004. Changing distribution of gender in the Extended Bangkok Region under globalization. *GeoJournal*, 61, 255-262. <https://doi.org/10.1007/s10708-004-3683-6>.
- Nguyen C.T., Chidthaisong A., Diem P.K., Huo L., 2021a. A Modified Bare Soil Index to Identify Bare Land Features during Agricultural Fallow-Period in Southeast Asia Using Landsat 8. *Land*, 10, 1-17. <https://doi.org/10.3390/land10030231>.
- Nguyen C.T., Nguyen D.T.H., Phan D.K., 2021b. Factors affecting urban electricity consumption: a case study in the Bangkok Metropolitan Area using an integrated approach of earth observation data and data analysis. *Environ. Sci. Pollut. Res.*, 28, 12056-12066. <https://doi.org/10.1007/s11356-020-09157-6>.
- Nitivattananon V., Srinonil S., 2019. Enhancing coastal areas governance for sustainable tourism in the context of urbanization and climate change in eastern Thailand. *Adv. Clim. Chang. Res.*, 10, 47-58. <https://doi.org/10.1016/j.accre.2019.03.003>.
- Pansuwan A., Routray J.K., 2011. Policies and pattern of industrial development in Thailand. *GeoJournal*, 76, 25-46. <https://doi.org/10.1007/s10708-010-9400-8>.
- Peng X., Chen X., Cheng Y., 2010. Urbanization and Its Consequences, in: Zheng, Y. (Ed.), *Demography. Encyloedia of Life Support Systems. Encyclopedia of Life Support Systems (EOLSS)*, UK, 210-235.
- Pruksanubal B., 2016. Land Use Transformation Process in Chachoengsao Province, Thailand. *Procedia Soc. Behav. Sci.*, 222, 772-781. <https://doi.org/10.1016/j.sbspro.2016.05.159>.
- Qiao K., Zhu W., Hu D., Hao M., Chen S., Cao S., 2017. Examining the distribution and dynamics of impervious surface in different functional zones of Beijing. *Dili Xuebao/Acta Geogr. Sin.*, 72, 2018-2031. <https://doi.org/10.11821/dlx201711008>
- Ramachandra T.V., Bharath A.H., Sowmyashree M.V., 2015. Monitoring urbanization and its implications in a mega city from space: Spatiotemporal patterns and its indicators. *J. Environ. Manage.*, 148, 67-81. <https://doi.org/10.1016/j.jenvman.2014.02.015>.
- Rawat J.S., Kumar M., 2015. Monitoring land use/cover change using remote sensing and GIS techniques: A case study of Hawalbagh block, district Almora, Uttarakhand, India. *Egypt. J. Remote Sens. Sp. Sci.*, 18, 77-84. <https://doi.org/10.1016/j.ejrs.2015.02.002>.
- Rubiera Morollón F., González Marroquín V.M., Pérez Rivero J.L., 2017. Urban sprawl in Madrid?: An analysis of the urban growth of Madrid during the last quarter of the twentieth century. *Lett. Spat. Resour. Sci.*, 10, 205-214. <https://doi.org/10.1007/s12076-016-0181-7>
- Shen W., Wu J., Grimm N.B., Hope D., 2008. Effects of urbanization-induced environmental changes on ecosystem functioning in the Phoenix metropolitan region, USA. *Ecosystems*, 11, 138-155. <https://doi.org/10.1007/s10021-007-9085-0>.
- Shouhai D., 2015. Employment in Township Urbanization in China. *Soc. Sci. China*, 36, 152-167. <https://doi.org/10.1080/02529203.2015.1029675>.
- Singh A., Kumar U., Seitz F., 2015. Remote sensing of storage fluctuations of poorly gauged reservoirs and state space model (SSM)-based estimation. *Remote Sens.*, 8, 17113-17134. <https://doi.org/10.3390/rs8110960>.
- Son N.T., Chen C.F., Chen C.R., 2020. Urban expansion and its impacts on local temperature in San Salvador, El Salvador. *Urban Clim.*, 32, 100617. <https://doi.org/10.1016/j.uclim.2020.100617>.
- Son N.T., Chen C.F., Chen C.R., Thanh B.X., Vuong T.H., 2017. Assessment of urbanization and urban heat islands in Ho Chi Minh City, Vietnam using Landsat data. *Sustain. Cities Soc.*, 30, 150-161. <https://doi.org/10.1016/j.scs.2017.01.009>.
- Son N.T., Thanh B.X., 2018. Decadal assessment of urban sprawl and its effects on local temperature using Landsat data in Cantho city, Vietnam.

- Sustain. Cities Soc., 36, 81-91. <https://doi.org/10.1016/j.scs.2017.10.010>.
- Song Y., Aryal J., Tan L., Jin L., Gao Z., Wang Y., 2021. Comparison of changes in vegetation and land cover types between Shenzhen and Bangkok. L. Degrad. Dev., 32, 1192-1204. <https://doi.org/10.1002/ldr.3788>.
- Stewart J.E., Battersby S.E., Lopez-De Fede A., Remington K.C., Hardin J.W., Mayfield-Smith K., 2011. Diabetes and the socioeconomic and built environment: Geovisualization of disease prevalence and potential contextual associations using ring maps. Int. J. Health Geogr., 10, 1-10. <https://doi.org/10.1186/1476-072X-10-18>.
- Sun W., Chen B., Messinger D.W., 2014. Nearest-neighbor diffusion-based pan-sharpening algorithm for spectral images. Opt. Eng., 53, 013107-1-11. <https://doi.org/10.1117/1.OE.53.1.013107>.
- Thanh L. Van, 2007. Economic development, urbanization and environmental changes in Ho Chi Minh city, Vietnam: Relations and policies, in: PRIPODE Workshop on Urban Population, Development and Environment Dynamics in Developing Countries. Nairobi, Kenya.
- Tolessa T., Senbeta F., Kidane M., 2017. The impact of land use/land cover change on ecosystem services in the central highlands of Ethiopia. Ecosyst. Serv., 23, 47-54. <https://doi.org/10.1016/j.ecoser.2016.11.010>.
- Tontisirin N., Phoomikiattisak D., Anantsuksomsri S., 2017. Land Use Change in the Eastern Economic Corridor of Thailand: An Application of Cellular Automata-Makov Model, in: The 54th Annual Meeting of the Japan Section of the RSAI, 1-7.
- Tran D.X., Pla F., Latorre-Carmona P., Myint S.W., Caetano M., Kieu H.V., 2017. Characterizing the relationship between land use land cover change and land surface temperature. ISPRS J. Photogramm. Remote Sens., 124, 119-132. <https://doi.org/10.1016/j.isprsjprs.2017.01.001>.
- Tsuchiya K., Hara Y., Thaitakoo D., 2015. Linking food and land systems for sustainable peri-urban agriculture in Bangkok Metropolitan Region. Landsc. Urban Plan., 143, 192-204. <https://doi.org/10.1016/j.landurbplan.2015.07.008>.
- Tucker C.J., 1979. Red and photographic infrared linear combinations for monitoring vegetation. Remote Sens. Environ., 8, 127-150. [https://doi.org/10.1016/0034-4257\(79\)90013-0](https://doi.org/10.1016/0034-4257(79)90013-0).
- United Nations, 2018. The World's Cities in 2018: Data Booklet. Population Division, Department of Economic and Social Affairs, United Nations, New York.
- Viera A.J., Garrett J.M., 2005. Understanding Interobserver Agreement: The Kappa Statistic. Fam. Med., 37, 360-363.
- Viet P.B., Thi T. Lan H., Phung H.P., 2014. Performance of Landsat 7 ETM+ Image in SLC-Off Mode for land cover classification, in: International Symposium on Geoinformatics for Spatial Infrastructure Development in Earth and Allied Sciences, 3-8.
- Watson D.F., 1992. Contouring. A guide to the analysis and display of spatial data. Oxford: Elsevier.
- Wulder M.A., Ortlepp S.M., White J.C., Maxwell S., 2008. Evaluation of Landsat-7 SLC-off image products for forest change detection. Can. J. Remote Sens., 34, 93-99. <https://doi.org/10.5589/m08-020>.
- Xinmin Z., Estoque R.C., Murayama Y., 2017. An urban heat island study in Nanchang City, China based on land surface temperature and social-ecological variables. Sustain. Cities Soc., 32, 557-568. <https://doi.org/10.1016/j.scs.2017.05.005>.
- Yamashita A., 2017. Bangkok Metropolitan Area, in: Murayama Y., Kamusoko C., Yamashita A., Estoque R.C. (Eds.), Urban Development in Asia and Africa. The Urban Book Series. Springer, Singapore, 151-169. <https://doi.org/10.1007/978-981-10-3241-7>.
- Zha Y., Gao J., Ni S., 2003. Use of normalized difference built-up index in automatically mapping urban areas from TM imagery. Int. J. Remote Sens., 24, 583-594. <https://doi.org/10.1080/01431160304987>.